CHINESE JOURNAL OF PHYSICS VOL. 38, NO. 2-II APRIL 2000

Flicker (1/f) Noise in 45± Bi-Epitaxial Grain Boundary Junctions and dc SQUID of $YBa_2Cu_3O_y$

B. C. Yao, S. H. Tsai, C. C. Chi, and M. K. Wu

Materials Science Center and Department of Physics, National Tsing Hua University, Hsinchu, Taiwan 300, R.O.C.

(Received August 17, 1999)

We have fabricated dc superconducting quantum interference devices (SQUIDs) incorporating 45° bi-epitaxial grain boundary junction, i.e. YBCO/YSZ and YBCO/YBCO/YSZ, in washer geometry. The $1/f$ noise power of single junction comes from resistance fluctuation for high current bias and critical current fluctuation for low current bias. The noise spectrum of the dc SQUIDs was measured with dc and ac bias schemes and showed value of $\sim 1\times10^{-5}$ $\Phi_0/\mathrm{Hz}^{1/2}$ at 100 Hz. The possible noise sources, critical current fluctuations, flux motion noise and resistance fluctuation, are investigated. The results are compared with previous published data.

PACS. 85.25.Cp – Josephson devices.
PACS. 85.25.Dq – Superconducting quantum interference devices (SQUIDs).

I. Introduction

The dc superconducting quantum interference device (SQUID) is currently the most sensitive detector for measuring magnetic flux. They are used in variety of applications. The sensitivity of dc SQUID is limited by noise which usually consist a temperature dependant white noise and low frequency $1/f$ noise [1, 2, 3]. Many high-T_c SQUIDs, exhibiting larger noise than low-T_c SQUIDs, have a serious limitation in many applications. To find out which type of SQUID has the lowest noise, to study and suppress different noise sources in the SQUIDs are task that are important for applications.

There is considerable progress in the fabrication and understanding of high-T_c SQUIDs. A number of weak-link superconductor-insulator-superconductor (SIS), grain boundary junctions, barrier and weakened junctions have been made with reliable I-V characteristics [4]. However, single-level dc-SQUIDs with grain-boundary junctions are the simplest to fabricate and appealing for practical applications. Although some studies of misorientation angles grain boundary junctions have been concluded [5], the properties of the high angle $(\sim 45^{\pm})$ grain boundary has not been clarified.

In this letter, we report an investigation of $1/f$ noise properties in a new structure $45^{\pm}$ bi-epitaxial grain boundary junctions and SQUIDs. The SQUIDs have a square-washer design and show the RSJ behavior, with a much higher J_c ($\sim 10^5$ A/cm^2) than other high angle grain boundary junctions and the $I_C R_N$ product is ~ 1 mV at 4.2 K.

II. Experimental procedures

The SQUIDs were based on YBCO grain boundary junction forms on Yttrium Stabilized Zirconia (YSZ) substrates. Details of the fabrication process were published elsewhere [6]. Briefly, the films were deposited by pulsed KrF excimer laser with $\lambda = 248$ nm. The first YBCO film was grown at 600 ±C by laser ablating a sintered YBCO target with the energy density about 1.5 J/cm^2 for thickness of 200 Å. The oxygen pressure during growth was 300 mtorr. After one side of low temperature grown YBCO film was removed by wet etching, the sample was then put back into chamber to grow high temperature YBCO film at 780 ±C. The in-plane epitaxial relationship between films and substrates was investigated by X-ray ϕ-scan. The corresponding ϕ-scan shows that the high temperature YBCO film (at 780 ±C) has a 0± in-plane rotation with respect to the YSZ substrate. While the low temperature YBCO film (at 600 ±C) has a 45± in-plane rotation with respect to the YSZ substrate due to large lattice mismatch. The junctions and SQUIDs were patterned by photolithography. The width of junction ~ 10 μm with typical normal resistance R_N of few and critical current I_0 of 200 μA to few mA at 4.2 K.

The electrical measurements were mainly carried out at 4.2 K with the samples immersed in liquid Helium. The cryostat was placed inside rf-shielding room. The I-V and noise were measured with four-point probes configuration. The noise voltage was amplified by a low noise bipolar pre-amplifier [7] which is connected to a HP3562 spectrum analyzer. The background voltage noise of the pre-amplifier was about 0.9 nV Hz$^{i\ 1/2}$ at 100 Hz and the $1/f$ corner frequency is ~ 3 Hz. For large current bias ($>$ few μA), the voltage noise contribution from pre-amplifier is negligible.

III. Results and discussion

In Fig. 1(a) we show a typical root mean square (rms) noise $S_V^{1/2}$ vs. frequency of a junction for different current bias. The spectral density of the noise from the junctions scaled approximately as $1/f$ at frequency below 100 Hz. Fig. 1(b) shows the rms noise $S_V^{1/2}$ (10 Hz) and the dynamic resistance of the junction vs. current bias. The critical current I_0 of the junction is about 150 μA. The variation of the $S_V^{1/2}$ (10 Hz) coincide with dynamic resistance R_{dyn} quite well. The noise shows a linear dependence on I at high bias current and sharp rise at bias current around I_0. To analyze the data quantitatively, we use the similar method of Ref. 8. The spectral density of the voltage noise without considering cross-spectral density of the the fluctuations δI_0 and δR is

$$S_V(f) = S_i(f)(V - IR_{dyn})^2 + S_r(f)V^2.$$

Where $R_{dyn} = \partial V/\partial I$, $S_i(f) = S_{I_0}(f)/I_0^2$, $S_r(f) = S_R/R^2$, The data were separated into those taken at high current and those taken at low bias. In Fig. 2 we plot $S_V^{1/2}$ (10 Hz) vs V^2 for high current bias and [$S_V^{1/2}$ (10 Hz) - $V^2 S_R/R^2$] vs. (V^2-IR_d) for the low current bias. We have excluded data from the noise-rounded region ($I < 6\pi k_B T/\Phi_0$) for the low bias current. It is clear that the data is close to a linear fit. We thus concluded that the noise is dominated by critical current fluctuation at low current bias and dominated by resistance fluctuations at high current bias. However, the value of $S_i(f)$ are much larger than $S_r(f)$ (i.e., $|\delta I_0/I_0| > |\delta R/R|$), which indicated a non uniform flow of current through the junction [8]. The atomic force microscopy

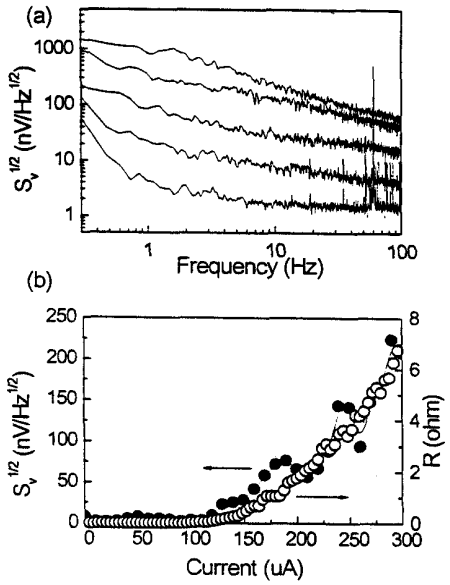

FIG. 1. (a) Root-mean-square voltage noise power vs. frequency of single junction. (b) Root-mean-square voltage noise power and dynamic resistance vs. bias current of single junction.

studies indicate facet structures between the junction suggesting that the current is distributed non-uniformly. The implication of facet structure and d-wave nature of YBCO will be published elsewhere.

The structure of square-washer SQUID used in our experiments has similar design as those of Ref. 3. In Fig. 3 we show I-V characteristic of the SQUID at 4.2 K. It shows RSJ-like I-V behavior with an $I_C R_N$ product ~ 1 mV. The I-V characteristic is asymmetric for positive and negative bias current. It is probably due to the different potential barrier height for forward and backward current bias. In Fig. 4(a) we plot the voltage versus applied magnetic field with different bias current. The modulation period corresponds exactly to one flux quantum in the SQUID loop. For large applied magnetic field, the modulation depth decreases due to magnetic field effect of the junction. The modulation period is slightly different for positive and negative applied magnetic field due to trapped flux in the junction. The modulation depth maximum is at bias current around 175 μA. The peak to peak value of output voltage is 130 μV, which is correspond to a transfer function $\partial V/\partial\Phi$ of 260 $\mu V/\Phi_0$. The calculated loop inductance is about 60 pH. The calculated dimensionless screen parameter $\beta = 2LI_0/\Phi_0 \sim 5$. In Fig. 4(b) shows the dependence of voltage-flux transfer function for different bias current. The maximum transfer function is at $I \sim I_0$. The voltage-flux characteristic deviated from sinusoidal behavior and modulation depth decreases with bias current away from I_0. In Fig. 5 we show flux noise power density spectra $S_\Phi (S_\Phi = S_V/V_\Phi,\ V_\Phi = \partial V/\partial\Phi)$ with 3 different bias currents. The rms flux noise $\Phi_n^{1/2}$ is $\sim 1 \times 10^{i\ 5}\ \Phi_0/\mathrm{Hz}^{1/2}$ at 100 Hz. The corresponding energy sensitivity of the SQUID is about ε (100 Hz) $\sim \Phi_n/2L \sim 3 \times 10^{i\ 30}$ J/Hz. At zero flux, noise power is scale $\sim 1/f$.

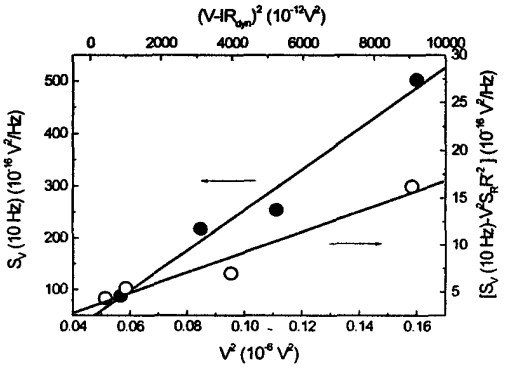

FIG. 2. $S_V^{1/2}$ (10 Hz) vs V^2 of single junction for high current and [$S_V^{1/2}$ (10 Hz)-$V^2 S_R/R^2$] vs ($V^2 - IR_d$) of single junction for low current.

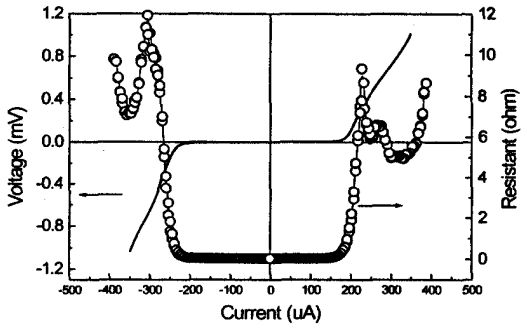

FIG. 3. IV characteristic and dynamic resistance of the square-washer SQUID.

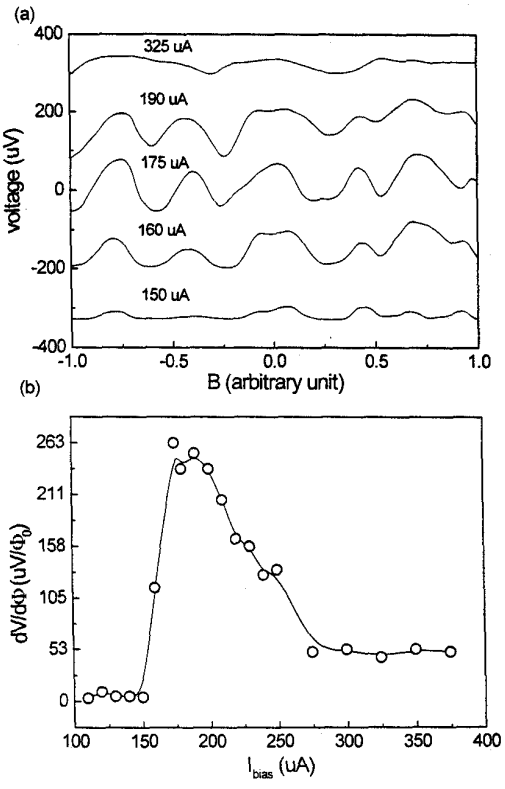

FIG. 4. (a) Voltage flux modulation with different bias current of the SQUID. (b) Transfer function vs. bias current.

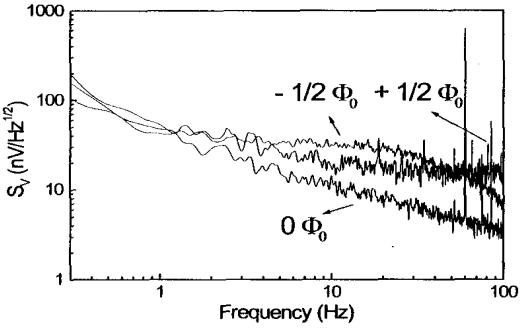

FIG. 5. Flux noise power of SQUID at 3 different flux.

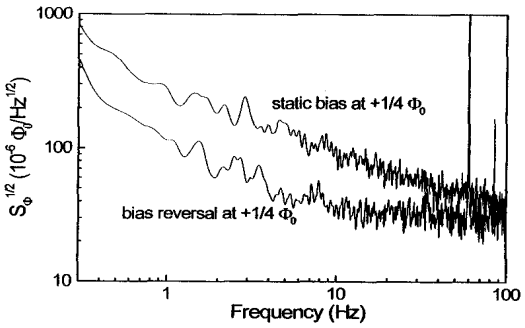

FIG. 6. Flux noise power with bias reversal.

However, at +0.5 flux quanta, the noise power is deviated from $1/f$. At -0.5 flux quanta, the noise observed was telegraphlike and the noise power is lorentzian, which can be associated with the flux motion in the film. The random telegraph noise was also observed at some particular current bias, which indicated carrier trapping at the junction interface. The noise power differences between the junction and the SQUID strongly suggests that the major part of the low frequency noise of SQUID originate from the flux noise in the YBCO film. The flux noise could come from the combination of asymmetric critical current fluctuation, asymmetric resistance fluctuation [9] and apparent flux fluctuation.

The importance question for the application of SQUID is whether or not the noise can be reduced by various methods. The frequent used method is bias-reversing method. In Fig. 6 shows bias reversal effect. A 400 Hz square-wave was applied to switch the junction bias between $+I$ and $-I$. A $1/f$ noise power reduction of about 2 times was observed when bias reversing. The observed noise reduction is similar with the result that suitable bias reversal schemes reduce the $1/f$ noise due to critical current or resistance fluctuation [8]. However, the noise reduction observed in our sample is less than other reports [2, 9]. The smaller reduction rules out critical current as a significant noise source, and combined with the results shown in Fig. 5, proves that apparent flux noise are the main $1/f$ noise source in our SQUID.

IV. Conclusion

In conclusion, we have fabricated new 45$^{\pm}$ bi-epitaxial grain boundary junction, SQUID and investigated their noise properties. It has been found that the $1/f$ noise of our high-T_c junction comes from resistance fluctuation for high current bias and critical current fluctuation for low current bias, while the $1/f$ noise of our high-T_c SQUID mainly comes from flux noise fluctuation. The high $I_C R_N$ product of the 45$^{\pm}$ bi-epitaxial grain boundary SQUID makes it suitable for practical application. However, the low noise reduction using bias reversal scheme indicate optimization of the junction interface is needed to reduce the apparent flux noise fluctuation.

References

[1] D. Koelle *et al*., Appl. Phys. Lett. **63**, 2271 (1993).
[2] M. I. Faley *et al*., Appl. Phys. Lett. **67**, 2087 (1995).
[3] R. Gross *et al*., Appl. Phys. Lett. **57**, 727 (1990).
[4] Harold Weinstock, *SQUID Sensors : Fundamentals, Fabrication and Applications* (Kluwer Academic Publishers, Dordrecht 1996).
[5] T. Minotani *et al*., Jpn. J. Appl. Phys. **37**, L718 (1998).
[6] Submitted to Physica C.
[7] D. Drung, Rev. Sci. Instrum. **68**, 4066 (1997).
[8] A. H. Miklich *et al*., Appl. Phys. Lett. **60**, 1899 (1992).
[9] R. H. Koch *et al*., Appl. Phys. Lett. **60**, 507 (1992).